

- Landscape position units (LSU) are adopted to identify priority management areas (PMAs).
- A Markov chain-based surrogate model of SWAT+ is proposed to identify PMAs.
- SWAT+ is qualified to provide flow distribution matrix among LSUs and channels.
- LSU-based PMAs are more effective in distribution and cumulative load contribution.
- LSU-based PMAs have general applicability for various geographic environments.

1 Identification of watershed priority management areas based on
2 landscape positions: an implementation using SWAT⁺

3
4
5 **Abstract**

6 Priority management areas (PMAs) of a watershed are areas with high
7 contributions to the pollutant load of the assessment outlet, such as the watershed outlet,
8 and thus, have high priority in the decision-making of comprehensive watershed
9 management. Existing spatial units used to identify PMAs are commonly based on three
10 concepts including subbasins, artificial geographic entities, and grid cells. However,
11 these identification units cannot balance the general applicability to diverse geographic
12 environments and the representation degree of spatial heterogeneity, which impacts the
13 effectiveness of the PMAs. This study proposes adopting landscape positions along the
14 hillslope as identification units of PMAs, which can be represented by slope position
15 units (e.g., upland, backslope, and valley). Landscape position units inherently have
16 upstream-downstream relationships with each other and with channels. Therefore, their
17 contributions to the assessment outlet can be quantified based on the propagation effects
18 of hillslope and channel routing processes. The proposed method was implemented
19 using a restructured and enhanced version of the Soil and Water Assessment Tool
20 (SWAT⁺), and an improved Markov chain-based surrogate model. Two watersheds, one
21 in China and one in the USA, with different geographic characteristics were selected to
22 separately conduct the comparative experiments to identify PMAs at the landscape
23 position and the subbasin levels. The results showed that PMAs based on landscape

24 positions have more accurate spatial distribution and require less area for the future
25 configuration of management practices to achieve the same management goal as PMAs
26 based on subbasins. The better effectiveness of landscape position units in identifying
27 PMAs is mainly due to their better ability to represent hillslope processes and the spatial
28 heterogeneity of underlying surface environments within subbasins. The proposed
29 method can be implemented by other watershed models that support landscape position
30 units or different types of spatial units with explicit upstream-downstream relationships
31 within subbasins.

32 **Keywords:** Priority management areas; Landscape positions; Spatial units;
33 Pollutant load contribution; Best Management Practices; SWAT⁺

1. Introduction

The priority management area (PMA) is a prioritizing area for management in the watershed, which has a high pollutant production, and more importantly, a high contribution to the pollutant load of its direct or indirect downstream water bodies (Chen et al., 2014). This concept is similar to the critical source area (CSA), which is more commonly used to identify highly polluted areas (Pionke et al., 2000; White et al., 2009) but usually does not emphasize propagation effects from upstream to downstream in the watershed, which is essential in the decision-making of comprehensive watershed management. Priority management areas are ideal spatial locations for implementing suitable best management practices (BMPs) to effectively control ecological and environmental problems, such as soil erosion and non-point source pollution (Shen et al., 2015; Tian et al., 2020; Guo et al., 2022). The identification of PMAs can be regarded as the first step in the spatial configuration of BMPs for comprehensive watershed management, where factors affecting actual management decisions, such as investment plans, stakeholders' willingness, environmental goals, and BMP effectiveness, could be considered. The spatial distribution of PMAs considerably affects the locations, areas, and effectiveness of the configured BMPs, affecting the cost-effectiveness of the BMP scenario (i.e., the spatial configuration of multiple BMPs in the watershed) (Chiang et al., 2014; Qin et al., 2018; Wang et al., 2016; Zhu et al., 2021). Therefore, the accurate identification of PMAs is a key issue for comprehensive watershed management (Chen et al., 2022).

22 The foremost step in identifying PMAs is to determine an appropriate type of
23 spatial units as a computing unit for pollutant production and contribution to the
24 assessment outlet, such as the watershed outlet (hereafter referred to as the
25 identification units) (Dong et al., 2018; White et al., 2009). The identification units
26 adopted in existing research are mainly based on three concepts: subbasins (Shang et
27 al., 2012; Chen et al., 2014; Shen et al., 2015; Dong et al., 2018), artificial geographic
28 entities (Tian et al., 2020), and grid cells (Kovacs et al., 2012).

29 The subbasin represents a relatively closed and independent geographic unit that
30 is linked to other subbasins through channels. Subbasin units are the most
31 straightforward and most frequently used identification units because they are
32 delineated and modeled in most watershed modeling. In addition to directly utilizing
33 subbasin units, researchers also use the combination of subbasins as identification units
34 according to administrative regions (such as villages; Shang et al., 2012), for the benefit
35 of making and implementing watershed management policies (Liu et al., 2019; Shang
36 et al., 2012). However, a subbasin can be recognized and modeled as an integral of one
37 or more levels of finer spatial units to better represent spatial heterogeneity within it,
38 such as hillslopes, slope position units, landuse fields, and even grid cells. Therefore, it
39 may be too coarse to use these subbasin-based identification units because the
40 heterogeneity of pollutant sources and transportation processes within the subbasins
41 should be considered (Qin et al., 2018; Wang et al., 2016).

42 Artificial geographic entities refer to artificially constructed and hydrologically
43 connected geographic entities based on the characteristics of a specific geographic

44 environment (Ghebremichael et al., 2013), such as polders that developed in lowland
45 plains with densely distributed rivers and lakes (Tian et al., 2020). Such spatial units
46 have relatively homogeneous features from the perspectives of physical geographic
47 processes and/or anthropogenic activities. For example, a polder may contain
48 agricultural land, irrigation channels, ponds, and even villages, that are enclosed by
49 artificial dams to serve as conservation areas for flood and waterlogging. Although
50 artificial geographic entities are appropriate for use as identification units in the
51 corresponding geographic environments, they are not easy to be generalized as
52 generally applicable identification units and are widely applied.

53 Grid cells are commonly used spatial units with regular shapes in geographic
54 modeling, and their underlying surface characteristics are homogeneous. Using
55 watershed models that explicitly represent flow routings among grid cells, PMAs can
56 be identified accurately (Kovacs et al., 2012). However, using grid cells may cause
57 more fragmented distributions of PMAs, which reduces the implementation
58 efficiency and limits further application (e.g., the PMA-based spatial optimization of
59 BMPs).

60 Therefore, the existing spatial units used for identifying PMAs cannot balance the
61 general applicability to diverse geographic environments and the representation degree
62 of spatial heterogeneity. According to the previous analysis, proper identification units
63 should (1) be broadly available and not be limited to a specific geographic environment;
64 (2) be capable of representing the spatial heterogeneity of underlying surface
65 characteristics, physical geographic processes, and/or anthropogenic activities inside

66 the study area by a small number of units; and (3) have hydrologic connections among
67 each other.

68 This study proposes the use of landscape positions along hillslopes within each
69 subbasin to identify PMAs. Landscape positions can be delineated by landform units
70 (also referred to as slope position units) that reflect the integrated effects of hillslope
71 processes on topography and affect geographic processes on the surface (Volk et al.,
72 2007; Arnold et al., 2010; Miller and Schaetzl, 2015; Qin et al., 2018). Landscape
73 position units are universality in most geographic environments (Wolock et al., 2004).
74 Based on commonly used classification systems of slope positions (e.g., the divide,
75 backslope, and valley units adopted by Arnold et al. (2010)), each subbasin needs only
76 a few spatial units (e.g., three) to represent the spatial homogeneity from the perspective
77 of hillslope processes (Qin et al., 2018; Rathjens et al., 2016). In addition, landscape
78 position units have inherent upstream-downstream relationships among each other,
79 which have been considered in watershed modeling (Arnold et al., 2010; Bieger et al.,
80 2019; Rathjens et al., 2015; Yang et al., 2002) and spatial optimization of BMPs (Qin
81 et al., 2018; Zhu et al., 2019; Zhu et al., 2021). Thus, landscape position units meet the
82 requirements for use as identification units mentioned above.

83 This study proposes a PMA identification method based on landscape position
84 units exemplified by SWAT⁺ (i.e., the restructured and enhanced version of the Soil and
85 Water Assessment Tool) and evaluates the effectiveness of the proposed method by
86 comparing it to widely used subbasin units. The remainder of this paper is organized as

87 follows: Section 2 introduces the proposed method; and Section 3 presents a

88 comparative experimental design of using landscape position and subbasin units to
89 identify PMAs of total nitrogen in two watersheds with different geographic
90 characteristics. The experimental results and discussion are presented in Section 4, and
91 the conclusions are presented in Section 5.

92 **2. Method design**

93 To identify PMAs at the landscape position unit level, two key issues must be
94 addressed. The first is the quantification of pollutants released at landscape position
95 units. The second is how to distinguish the pollutant load contribution of each landscape
96 position unit to the assessment outlet, that is, the residual amount of pollutant after
97 being transported to its direct downstream channel and then transitioning in hierarchical
98 channels before reaching the assessment outlet (Chen et al., 2014).

99 Generally, the contribution of the pollutant load cannot be directly determined
100 from the results of most watershed models. Instead, watershed models output the
101 pollutant released from each simulation unit (e.g., the hydrologic response unit [HRU]
102 in SWAT) or lumped unit (e.g., subbasin), as well as the flow of substances in and out
103 of each channel. To fill this gap, Grimvall and Stålnacke (1996) proposed a Markov
104 chain-based surrogate model to simulate pollutant transitions from upstream channels
105 (one channel for each subbasin) to the assessment outlet in a statistical manner. Their
106 basic idea is to use analog pollutant transformation and transfer processes in
107 hierarchical channels as a Markov process, in which, the transition matrix is determined
108 by the upstream-downstream relationships among channels and the retention effects of

109 the channel routing process. After a finite number of transitions (equal to the length of
110 the longest branch in hierarchical channels), all pollutants from upstream subbasins
111 reach the assessment outlet, thus, the corresponding pollutant load contributions can be
112 derived (Grimvall and Stålnacke, 1996).

113 Follow-up studies continued to adopt the subbasin unit in the Markov chain-based
114 model (Chen et al., 2014; Rankinen et al., 2016), which includes pollutant production
115 at hillslopes and pollutant routing in the channel. The transition matrix of the Markov
116 chain-based model can be improved to represent both landscape position and channel
117 units. Therefore, if we can separate these two processes in landscape position units and
118 channels, the improved Markov chain-based model will be able to distinguish the
119 pollutant contribution of each landscape position unit to the assessment outlet. Based
120 on this basic idea, the proposed method aims to incorporate a watershed model that
121 supports landscape position units as simulation or lumped units, to improve the Markov
122 chain-based PMA identification method from the subbasin level to the landscape
123 position unit level. Therefore, the Markov chain-based PMA identification method can
124 be generalized as a method framework that supports one or more types of hierarchical
125 spatial units with explicit hydrological connections (i.e., upstream-downstream
126 relationships), such as subbasins and landscape position units (Fig. 1).

127 **2.1 Delineation and modeling of landscape position units in SWAT⁺**

128 As a restructured and enhanced version of the SWAT model, SWAT⁺ (Bieger et al.,
129 2017, 2019) introduced a new type of spatial unit between the subbasin unit and HRU
130 named the landscape position unit (LSU), which includes the uplands and floodplains

131 (Fig. 2). This means that the basic spatial discretization of a watershed in SWAT⁺
132 contains three types of nested spatial units as a hierarchy: subbasin, LSU, and HRU. In
133 addition, SWAT⁺ also abstracts specific types of geographic entities as spatial units with
134 locations and properties to participate in watershed modeling. For example, reservoirs
135 or ponds within a subbasin are first generalized as one point in the channel that divides
136 the channel into two parts, and then defined by the upstream part with additional
137 properties such as storage capacity (Fig. 2). The hillslopes, LSUs, and HRUs are also
138 delineated accordingly, while the two aquifer units remain unchanged (Fig. 2). These
139 spatial units can enrich the flow routing network of SWAT⁺ and play important roles in
140 the simulation of study areas with specific geographic environments, such as,
141 agricultural ecosystems with densely distributed ponds.

142 With the new spatial discretization scheme, SWAT⁺ improved the representation
143 of realistic hydrologic processes from hillslopes to channels (Bieger et al., 2019).
144 Instead of directly adding all released substances of HRUs (including water, sediment,
145 and pollutants) to the channel, SWAT⁺ first lumps HRUs' outputs at the LSU level and
146 then routes to other spatial units using two different methods. The first method involves
147 completely draining from the upland to the floodplain and from the floodplain to the
148 channel, which is applicable for lateral flow in soils and groundwater recharge in
149 aquifers (Fig. 2). The second method distributes water from the upland to the
150 channel/pond/reservoir by a constant ratio (e.g., 0.30 from LSU2 to the pond and 0.66
151 from LSU4 to the channel, as shown in Fig. 2; hereafter 'channel/pond/reservoir' is
152 referred to as channel collectively) and the rest to the floodplain as additional net

153 precipitation to participate in the simulation. The output from the floodplain drains
154 entirely into the channel (Fig. 2). SWAT⁺ provides two ways to determine this ratio: the
155 user-specified global value for all upland units in the watershed and the area ratio of
156 each upland to its floodplain. The area ratio method has been proven to be more realistic
157 in representing the connectivity than the fixed ratio for the entire watershed (Bieger et
158 al., 2019) and is therefore adopted in this study.

159 With the flow routing network primarily constructed by HRU, LSU, and channel
160 (Fig. 2), SWAT⁺ is qualified to quantify pollutants released at landscape position units
161 and the corresponding transportation amounts to their direct channels.

162 **2.2 Pollutant load contribution of landscape position units derived** 163 **from a Markov chain-based surrogate model of SWAT⁺**

164 Based on the flow routing network and simulation results of SWAT⁺, the key part
165 of the Markov chain-based surrogate model can be determined, that is, the transition
166 matrix of pollutants through LSUs and channels. Subsequently, using the lumped
167 simulation results at LSUs as inputs, the Markov chain-based model can determine the
168 pollutant load contribution of each landscape position unit.

169 **2.2.1 Transition matrix of pollutants based on flow routing** 170 **network and retention effects of channel routing process**

171 The transition matrix is constructed using flow distribution relationships from
172 upstream to downstream units and the retention coefficients of channel routing
173 processes (Chen et al., 2014). According to the spatial discretization scheme of SWAT⁺

174 (see Section 2.1), the flow distribution relationships among the LSUs and channels can
 175 be represented by an $n \times n$ matrix H (Eq. 1). Fig. 3 shows an example of the matrix H .

$$176 \quad H(i,j) = \begin{cases} s, & \text{if LSU (floodplain) } j \text{ is adjacent downstream of LSU (upland) } i \\ 1-s, & \text{if CHA (channel) } j \text{ is direct downstream of LSU (upland) } i \\ 1, & \text{if CHA } j \text{ is adjacent downstream of CHA } i \text{ or LSU (upland) } i \\ 0, & \text{otherwise} \end{cases} \quad (1)$$

177 where n is the total number of LSUs and channels in the watershed, and s is the flow
 178 distribution ratio from upland to floodplain. For surface runoff, s is initially set by the
 179 area ratio of upland and hillslope, while for lateral flow and groundwater recharge, $s =$
 180 1 (Fig. 2). Each row represents the flow distribution relationships of a spatial unit with
 181 its downstream units. The sum of all elements in one row equals 1, except for the
 182 channel row where the assessment outlet is located (e.g., the 7th row in Fig. 3, when the
 183 outlet of channel 7 is the assessment outlet). For a given assessment outlet of channel
 184 k , there exists a smallest integer N_k to make $H^{N_k} = 0$, which means that after N_k
 185 transitions, pollutants from all upstream spatial units of channel k will reach the outlet.
 186 The physical meaning of N_k is the longest routing length from the uppermost spatial
 187 units to the outlet of channel k , for example, $N_7 = 4$ in Fig. 3.

188 The complicated channel routing process accounting for pollutant transformation
 189 and transfer processes can be simplified by using a retention coefficient (i.e., removal
 190 capacity of pollutants) as a surrogate calculation method (Chen et al., 2014; Grimvall
 191 and Stålnacke, 1996; Hejzlar et al., 2009). The landscape position unit is a lumped unit
 192 of pollutant sources calculated at HRUs, thus, has no retention effect. The retention
 193 coefficient R is also represented by an $n \times n$ matrix, as follows:

194

$$R = \begin{pmatrix} r_1 & 0 & \cdots & 0 \\ 0 & r_2 & \cdots & 0 \\ \vdots & \vdots & \ddots & \vdots \\ 0 & 0 & \cdots & r_n \end{pmatrix} \quad (2)$$

195 Where the i th diagonal element r_i denotes the retention coefficient of spatial unit i ; for
 196 LSUs, $r_i = 0$; and for channels, r_i can be calculated using the simulation results of
 197 channels:

198

$$r_j = (\text{Load}_{\text{in}} - \text{Load}_{\text{out}}) / \text{Load}_{\text{in}} \quad (3)$$

199 where Load_{in} is the pollutant input to channel j that includes pollutant outputs of
 200 adjacent upstream channels and pollutant released from upstream LSUs; and Load_{out} is
 201 the pollutant output at the outlet of channel j .

202 The transition matrix \tilde{H} of the Markov chain-based model can be represented as
 203 follows and used to simulate the flow transitions of substances (e.g., water and
 204 pollutants) through the hierarchy of landscape position units and channels:

205

$$\tilde{H} = H (I - R) \quad (4)$$

206 where I is an identity matrix.

207 **2.2.2 Calculation of pollutant load contribution**

208 Except for the transition matrix, the pollutant released from each LSU is the
 209 primary input data for the Markov chain-based model as the initial states. Because the
 210 channel acts as a receptor for pollutants, it contains no self-generated pollutants. An n
 211 $\times 1$ matrix L is used to organize the input of the pollutant sources:

212

$$L = (e_1, e_2, \cdots, e_i, \cdots, e_n)^T \quad (5)$$

213 where e_i is the pollutant released from spatial units i based on the simulation results of

214 SWAT⁺. Specifically, $e_i = 0$, if i is a channel.

215 The pollutant load contribution of each spatial unit to a specific assessment outlet
 216 can be calculated using simple matrix calculations (Grimvall and Stålnacke, 1996):

$$217 \quad E = (\tilde{H}_k)^{N_k} V_k * L \quad (6)$$

$$218 \quad \tilde{H}_k(i, j) = \begin{cases} \tilde{H}(i, j), & \text{if } i \neq k \\ 1, & \text{if } i = j = k \\ 0, & \text{if } i = k \text{ and } j \neq k \end{cases} \quad (7)$$

$$219 \quad V_k(i) = \begin{cases} 1, & \text{if } i = k \\ 0, & \text{otherwise} \end{cases} \quad (8)$$

220 where k represents the assessment outlet located channel, and the corresponding
 221 modification from \tilde{H} to \tilde{H}_k implies that the k th state is transformed to an absorbing
 222 state. V_k is an $n \times 1$ matrix for extracting the k th column of the $(\tilde{H}_k)^{N_k}$, resulting in
 223 the contribution rate of each unit. The asterisk* denotes element-wise multiplication.

224 Considering that pollutants of interest may have various states that are modeled in
 225 different watershed processes, the calculation of pollutant load contribution should be
 226 combined with all components calculated by different transition matrix H and pollutant
 227 source matrix L . For example, the total nitrogen considered in this study mainly
 228 includes nitrate nitrogen (NO_3) and the organic nitrogen ($ORGN$). Therefore, the total
 229 nitrogen load contribution can be calculated as follows:

$$230 \quad E_{TN} = E_{NO_3-SURF} + E_{NO_3-LAT} + E_{NO_3-GW} + E_{ORGN} \quad (9)$$

$$231 \quad E_{NO_3-SURF} = (H_{SURF}(I - R_{NO_3})_k)^{N_k} V_k * L_{NO_3-SURF} \quad (10)$$

$$232 \quad E_{NO_3-LAT} = (H_{LAT}(I - R_{NO_3})_k)^{N_k} V_k * L_{NO_3-LAT} \quad (11)$$

$$233 \quad E_{NO_3-GW} = (H_{GW}(I - R_{NO_3})_k)^{N_k} V_k * L_{NO_3-GW} \quad (12)$$

$$234 \quad E_{ORGN} = (H_{SURF}(I - R_{ORGN})_k)^{N_k} V_k * L_{ORGN-SURF} \quad (13)$$

235 where *SURF* denotes the surface runoff, *LAT* denotes the lateral flow, *GW* denotes the
236 groundwater recharge; H_{SURF} , H_{LAT} , and H_{GW} describe the flow distribution
237 relationships among the spatial units of surface runoff, lateral flow, and groundwater
238 recharge, respectively; $L_{NO3-SURF}$, $L_{NO3-LAT}$, and L_{NO3-GW} are the amounts of NO_3 released
239 in surface runoff, lateral flow, and groundwater recharge, respectively; and $L_{ORGN-SURF}$
240 is the amount of *ORGN* released in surface runoff.

241 **2.2.3 PMA identification based on classification of pollution** 242 **degrees**

243 Once the pollutant load contribution of each landscape position unit is
244 distinguished, a classification of pollution degrees can be adopted to identify different
245 levels of PMAs, such as high-, medium-, and low-contribution PMAs. The
246 classification methods in existing studies include the natural breaks method, standard
247 deviation method, and water quality control targets method (Chen et al., 2014; Giri et
248 al., 2016).

249 **3. Experimental design**

250 To illustrate the effectiveness of the proposed method, a comparative experimental
251 study was designed to identify the PMAs of total nitrogen at the landscape position and
252 subbasin levels based on the same calibrated SWAT⁺ model. The same experimental
253 design was used in two watersheds to evaluate the applicability of the method under
254 different geographic characteristics (e.g., topographical, climatic, hydrological, and

255 ecological conditions), that is, the Zhongtianshe Watershed (~42 km²) in southern
256 China and the Willow River Watershed (~212 km²) in western Wisconsin, USA (Fig.
257 4).

258 **3.1 Study areas and data**

259 The Zhongtianshe Watershed, located in the south of Liyang City, Jiangsu
260 Province, China, is a typical hilly area situated in the upstream region of Lake Tai. The
261 study area is characterized by a subtropical monsoon climate. The average annual
262 temperature is 15.5°C and the average annual precipitation is 1160 mm. The main soil
263 type is yellow-red soil, which is a type of acidic soil that is easily weathered. The main
264 land use types were forests (77%), croplands (10%, primarily paddy fields), orchards
265 (3%), residential areas (8%), and water areas (2%). The watershed experiences frequent
266 agricultural activities, and the cultivation of rice and wheat is the primary contributor
267 to local non-point source pollution. Because the study area is on the drinking water
268 source of Liyang, knowing the details of the pollution situation and taking reasonable
269 measures to control is a vital issue for the local government (Shi et al., 2021).

270 The Willow River, located in western Wisconsin, USA, is a tributary of the St.
271 Croix River. It is classified as the Central Wisconsin Undulating Till Plain based on a
272 report by the environmental protection agency (EPA, 2020), and is characterized as
273 relatively flat compared to the Zhongtianshe watershed. The area has a continental
274 climate with high evapotranspiration, an average annual temperature of 11.8°C, and an
275 average annual precipitation of 788 mm. The soils are predominantly silt loams with
276 moderately well-drained characteristics. The main land use types were grasslands

277 (45%), forests (27%), croplands (18%), residential areas (6%), and wetlands (3%).
278 Watershed crops are dominated by corn-silage, soybeans, and alfalfa, resulting in non-
279 point source pollution and relatively poor water quality. As the headwater of the popular
280 Willow River State Park and attractive trout fishing destinations, the watershed has
281 been the focus of non-point source pollution control for decades (Almendinger and
282 Murphy, 2007).

283 The input data of the study areas for SWAT⁺ modeling consisted of a digital
284 elevation model (DEM), land use types, soil types and properties, meteorological data,
285 agricultural management practices, and observed data at the watershed outlet. Detailed
286 descriptions of the data for the two watersheds are presented in Table 1.

287 **3.2 Modeling and calibration of the SWAT⁺ model**

288 Two SWAT⁺ models (version 59.3) were built to simulate the total nitrogen
289 pollution in each study area. A total of 15 subbasins, 41 LSUs, and 1260 HRUs were
290 generated in the Zhongtianshe Watershed, while 19 subbasins, 131 LSUs, and 7245
291 HRUs were generated in the Willow River Watershed (Fig. 5).

292 Limited by the available observed data of the Zhongtianshe Watershed, we set the
293 year 2011 as a warm-up period, and 2012–2013 and 2014–2015 as calibration and
294 validation periods for daily flow modeling. The model performance of the total nitrogen
295 was calibrated using only 5-day monitoring data from 2014 to 2015, without validation.

296 For the Willow River watershed, the model had a 2-year warm-up period. The
297 calibration period ranged from 1 January 2012 to 31 July 2014, and the validation
298 period was from 1 October 2010 to 31 December 2011, respectively. The available daily

299 ammonia and organic nitrogen were combined to calibrate and validate the nitrogen
300 modeling.

301 Model performance was evaluated using the Nash–Sutcliffe efficiency (NSE,
302 Nash and Sutcliffe, 1970), percentage bias (PBIAS), root mean square error-standard
303 deviation ratio (RSR), and R^2 , as listed in Table 2. According to the criteria of monthly
304 model performance proposed by Moriasi et al. (2007), calibrated SWAT⁺ models have
305 approximately satisfactory performance for flow modeling in both study areas. For
306 nitrogen, considering that a shorter time step may cause poorer model performance
307 (Engel et al. 2007), and that the simulation trend (shown in R^2) was quite consistent
308 with the observed data, we believe that both calibrated models are applicable for the
309 validation of the proposed PMA identification method in this study.

310 **3.3 Identification and evaluation of PMAs at LSU level and subbasin** 311 **level**

312 To evaluate the effectiveness of the PMAs at the LSU level, PMAs were also
313 identified at the subbasin level in the same study area based on the same calibrated
314 SWAT⁺ model and the original Markov chain-based surrogate model.

315 The average annual total nitrogen modeled during the calibration period was used
316 to identify the PMAs, with the watershed outlet set as the assessment outlet. The natural
317 break method was adopted to classify the nitrogen load contribution of the spatial units
318 into three classes, and high-contribution areas were identified as PMAs.

319 The comparison of PMAs identified at the LSU and subbasin levels was conducted
320 from two perspectives, the spatial distribution and cumulative load contributions. The

321 spatial distribution of PMAs is an intuitive way to qualitatively analyze the spatial
322 consistency and differences between different units. The cumulative load contributions
323 were used to quantitatively compare the relationships between the areas of PMAs and
324 their total pollutant load contribution.

325 **4. Experimental results and discussion**

326 **4.1 Spatial distribution of PMAs**

327 In the Zhongtianshe Watershed, five LSUs and two subbasins, classified as high-
328 contribution areas, were identified as PMAs (Fig. 6). There was a relatively consistent
329 spatial correlation between the two levels. For example, one subbasin was identified as
330 PMA at both levels, that is, subbasin S2 in Fig. 6b and its two LSUs, L2 and L3 in Fig.
331 6a. PMAs identified at the LSU level had a more accurate spatial distribution because
332 of the inherent characteristics of the LSUs that can represent the spatial heterogeneity
333 within subbasins. Considering the retention effect of ponds and reservoirs in SWAT⁺,
334 the upstream part of the subbasin may have a distinctive load contribution compared to
335 the downstream part. For example, in the subbasin S1 in Fig. 6b, the upstream part
336 constituted by floodplain L10 and upland L12 in Fig. 6a were identified as medium-
337 contribution areas, while the downstream floodplain L1 was the high-contribution area.
338 In addition, most LSU-based PMAs were floodplains in the Zhongtianshe Watershed.
339 This may be because that the cropland in the study area is mostly distributed along the
340 valley plain, which is a direct cause of local non-point source pollution. These results
341 also prove that SWAT⁺ is well suited for characterizing pollutants released at the LSU

342 level and their transitions in the reconstructed routing network by LSUs and channels
343 (including ponds).

344 In the Willow River Watershed, two LSUs and two subbasins, classified as high-
345 contribution areas, were identified as PMAs (Fig. 7). It was similar at both the LSU and
346 subbasin levels where the northeast areas of the watershed were identified as low
347 contribution areas, owing to the upstream pollution predominantly reduced by the
348 ponds and wetlands along the main channel. Although the results identified at the two
349 levels had similar spatial distributions, the subbasin-based PMAs covered larger areas
350 than the LSU-based PMAs, which may result in additional screening work or more
351 investment in watershed management decision-making. In contrast, the LSU-based
352 PMAs were the upland areas within the subbasins, that is, uplands L1 and L2 (Fig. 7a)
353 within two subbasins (Fig. 7b). The medium-contribution areas identified at the LSU
354 level were also more specific and detailed than the areas identified at the subbasin level.
355 Therefore, it is clear that LSU-based results can provide a finer identification than
356 subbasin-based results in the Willow River Watershed.

357 In addition, for the Willow River Watershed, LSUs belonging to subbasin L2 in
358 Fig. 7b were not identified as PMAs but as contribution areas below medium-
359 contribution areas. This shows that the application of detailed spatial units could
360 decompose the aggregation of the pollutant load within a subbasin in a relatively
361 realistic representation, although subbasin S2 contributed a high pollutant load as the
362 result of the largest subbasin in the watershed.

363 Overall, LSU-based PMAs have improved the accuracy of identification from the

364 perspective of spatial distribution compared with subbasin-based PMAs. It is also
365 proven that the proposed PMA identification method at landscape position units using
366 SWAT⁺ is effective and applicable to different watersheds.

367 **4.2 Cumulative load contribution**

368 To quantitatively evaluate the difference in PMAs identified at the LSU and
369 subbasin levels for each case study, each type of spatial unit was ranked by load
370 contribution in descending order and plotted in Figs. 8 and 9, with the cumulative area
371 and load contribution calculated.

372 In the Zhongtianshe Watershed, LSU-based PMAs contributed 48.6% of the total
373 nitrogen in 23.3% of the watershed area, whereas subbasin-based PMAs only
374 contributed 44.7% in as much as 30.1% of the area (Fig. 8a). This means that landscape
375 position units are more effective in identifying the PMAs. Moreover, the cumulative
376 area-contribution line of the LSU-based method in Fig. 8a was always higher than that
377 of the subbasin-based method, proving its better effectiveness, although based on
378 different types of identification units.

379 In the Willow River Watershed, LSU-based PMAs contributed 31.7% of the total
380 nitrogen in 5.9% of the watershed area, whereas subbasin-based PMAs contributed 54.9%
381 of the total nitrogen in 21.5% of the area (Fig. 9a). It is not convincing to simply use
382 these numbers to compare the effectiveness of the two levels in this watershed.
383 However, the line in Fig. 9a shows that the LSU-based PMAs almost always covered
384 less area than the subbasin-based PMAs under the same cumulative contribution. In
385 general, the results revealed that there would be less work on the reduction of pollution

386 at the LSU level if the local government wanted to control the pollution to a certain
387 extent.

388 Furthermore, there was no deterministic relationship between the area of the
389 spatial unit and its pollutant load contribution. For example, LSU L1 in the
390 Zhongtianshe Watershed contributed 12.0% of the total nitrogen but ranked 17 in area,
391 while subbasin S1 contributed 24.3% of the total nitrogen with the 2nd largest area (Fig.
392 8). In the Willow River Watershed, LSU L1 contributed 16.8% of total nitrogen with
393 the 2nd largest area, and subbasin S1 contributed 31.7% of total nitrogen which has the
394 2nd largest area of all subbasins (Fig. 9).

395 In summary, identifying PMAs based on landscape positions performs better than
396 subbasins from the perspectives of both the spatial distribution and cumulative load
397 contribution in both watersheds. Thus, LSU-based PMAs have the merit of accounting
398 for more pollutant load contributions with smaller areas, and can effectively be utilized
399 in the spatial configuration of BMPs for integrated watershed management.

400 **5. Conclusions**

401 This study proposes the use of landscape position units (LSUs), derived from a
402 universal type of spatial unit for most geographic environments, as identification units
403 for priority management areas (PMAs). An improved Markov chain-based surrogate
404 model of the SWAT⁺ model was implemented to distinguish the pollutant load
405 contribution of each LSU to the assessment outlet and then identify the PMAs according
406 to a classification method. Experimental results show that landscape position units are

407 more effective than widely used subbasins in identifying PMAs because of their
408 superior ability to represent hillslope processes and the spatial heterogeneity of
409 underlying surface environments within subbasins. Therefore, LSU-based PMAs are
410 much more valuable for providing accurate locations for implementing suitable BMPs
411 for integrated watershed management.

412 The improved Markov chain-based PMA identification method can be regarded as
413 a method framework. More types of spatial units with explicit upstream-downstream
414 relationships may be proposed and validated to identify PMAs with the support of
415 proper watershed models. In addition, several issues may be worth attention in future
416 research such as 1) how to consider various climate scenarios to determine the retention
417 effects of channel routing processes; 2) how to better quantify the hydrological
418 connectivity among landscape positions and channels and its effects on PMA
419 identification; 3) how a specific type of identification unit affects the identification of
420 PMAs under different delineation methods; 4) how the modeling accuracy and
421 precision of the same or different watershed models affects PMA identification; and 5)
422 how PMAs derived from different identification units impact the effectiveness and
423 efficiency of the spatial optimization of BMPs.

424 **Acknowledgement**

425 Supports to A-Xing Zhu through the Vilas Associate Award, the Hammel Faculty
426 Fellow Award, and the Manasse Chair Professorship from the University of Wisconsin-
427 Madison are greatly appreciated.

428 **Funding**

429 The work reported here was supported by grants from National Natural Science
430 Foundation of China (Project No.: 41871362, 42101480, 41871300) and the 111
431 Program of China (Approved Number: D19002).

432 **References**

433 [Almendinger, J.E., Murphy, M.S., 2007. Constructing a SWAT model of the Willow River watershed,](#)
434 [western Wisconsin. St. Croix Watershed Research Station, Science Museum of Minnesota. 84 pp.](#)

435 Arnold, J., Allen, P., Volk, M., Williams, J.R., Bosch, D., 2010. Assessment of different representations
436 of spatial variability on SWAT model performance. *Transactions of the ASABE*. 53(5), 1433–1443.
437 <https://doi.org/10.13031/2013.34913>.

438 Bieger, K., Arnold, J.G., Rathjens, H., White, M.J., Bosch, D.D., Allen, P.M., 2019. Representing the
439 connectivity of upland areas to floodplains and streams in SWAT+. *J. Am. Water Resour. Assoc.*
440 55(3), 578–590. <https://doi.org/10.1111/1752-1688.12728>.

441 Bieger, K., Arnold, J.G., Rathjens, H., White, M.J., Bosch, D.D., Allen, P.M., Volk, M., Srinivasan, R.,
442 2017. Introduction to SWAT+, a completely restructured version of the Soil and Water Assessment
443 Tool. *J. Am. Water Resour. Assoc.* 53(1), 115–130. <https://doi.org/10.1111/1752-1688.12482>.

444 Chen, L., Li, J., Xu, J., Liu, G., Wang, W., Jiang, J., Shen, Z., 2022. New framework for nonpoint source
445 pollution management based on downscaling priority management areas. *J. Hydrol.* 606, 127433.
446 <https://doi.org/10.1016/j.jhydrol.2022.127433>.

447 Chen, L., Zhong, Y., Wei, G., Cai, Y., Shen, Z., 2014. Development of an integrated modeling approach
448 for identifying multilevel non-point-source priority management areas at the watershed scale. *Water*

449 Resour. Res. 50(5), 4095–4109. <https://doi.org/10.1002/2013WR015041>.

450 Chiang, L.C., Chaubey, I., Maringanti, C., Huang, T., 2014. Comparing the selection and placement of
451 best management practices in improving water quality using a multiobjective optimization and
452 targeting method. *Int. J. Environ. Res. Public Health* 11(3), 2992–3014.
453 <https://doi.org/10.3390/ijerph110302992>.

454 Dong, F., Liu, Y., Wu, Z., Chen, Y., Guo, H., 2018. Identification of watershed priority management areas
455 under water quality constraints: A simulation-optimization approach with ideal load reduction. *J.*
456 *Hydrol.* 562, 577–588. <https://doi.org/10.1016/j.jhydrol.2018.05.033>.

457 Engel, B., Storm, D., White, M., Arnold, J., Arabi, M., 2007. A hydrologic/water quality model
458 application protocol. *J. Am. Water Resour. Assoc.* 43(5), 1223–1236. [https://doi.org/10.1111/j.1752-](https://doi.org/10.1111/j.1752-1688.2007.00105.x)
459 [1688.2007.00105.x](https://doi.org/10.1111/j.1752-1688.2007.00105.x).

460 [EPA. 2022. U.S. Environmental Protection Agency. Level III and IV ecoregions of the continental](#)
461 [environmental probability. Available online at \[https://www.epa.gov/eco-research/level-iii-and-iv-\]\(https://www.epa.gov/eco-research/level-iii-and-iv-ecoregions-state\)](#)
462 [ecoregions-state, last updated on May 2, 2022.](#)

463 Ghebremichael, L.T., Veith, T.L., Hamlett, J.M., 2013. Integrated watershed- and farm-scale modeling
464 framework for targeting critical source areas while maintaining farm economic viability. *J. Environ.*
465 *Manage.* 114, 381–394. <https://doi.org/10.1016/j.jenvman.2012.10.034>.

466 Giri, S., Qiu, Z., Prato, T., Luo, B., 2016. An integrated approach for targeting critical source areas to
467 control nonpoint source pollution in watersheds. *Water Resour. Manage.* 30, 5087–5100.
468 <https://doi.org/10.1007/s11269-016-1470-z>.

469 Grimvall, A., Stålnacke, P., 1996. Statistical methods for source apportionment of riverine loads of
470 pollutants. *Environmetrics* 7(2), 201–213.

471 095X(199603)7:2<201::AID-ENV205>3.0.CO;2-R.

472 Guo, Y., Wang, X., Melching, C., Nan, Z., 2022. Identification method and application of critical load
473 contribution areas based on river retention effect. *J. Environ. Manage.* 305, 114314.
474 <https://doi.org/10.1016/j.jenvman.2021.114314>.

475 Hejzlar, J., Anthony, S., Arheimer, B., Behrendt, H., Bouraoui, F., Grizzetti, B., Groenendijk, P., Jeuken,
476 M.H.J.L., Johnsson, H., Lo Porto, A., Kronvang, B., Panagopoulos, Y., Siderius, C., Silgram, M.,
477 Venohr, M., Žaloudík, J., 2009. Nitrogen and phosphorus retention in surface waters: an inter-
478 comparison of predictions by catchment models of different complexity. *J. Environ. Monit.* 11(3),
479 584. <https://doi.org/10.1039/b901207a>.

480 Kovacs, A., Honti, M., Zessner, M., Eder, A., Clement, A., Blöschl, G., 2012. Identification of
481 phosphorus emission hotspots in agricultural catchments. *Sci. Total Environ.* 433, 74–88.
482 <https://doi.org/10.1016/j.scitotenv.2012.06.024>.

483 Liu, G., Chen, L., Wei, G., Shen, Z., 2019. New framework for optimizing best management practices at
484 multiple scales. *J. Hydrol.* 578, 124133. <https://doi.org/10.1016/j.jhydrol.2019.124133>.

485 Miller, B.A., Schaetzl, R.J., 2015. Digital classification of hillslope position. *Soil Sci. Soc. Am. J.* 79(1),
486 132–145. <https://doi.org/10.2136/sssaj2014.07.0287>.

487 Moriasi D. N., Arnold J. G., Van Liew M. W., Bingner R. L., Harmel R. D., Veith T. L., 2007. Model
488 evaluation guidelines for systematic quantification of accuracy in watershed simulations.
489 *Transactions of the ASABE.* 50(3), 885–900. <https://doi.org/10.13031/2013.23153>.

490 Nash, J.E., Sutcliffe, J.V., 1970. River flow forecasting through conceptual models part I — A discussion
491 of principles. *J. Hydrol.* 10(3), 282–290. [https://doi.org/10.1016/0022-1694\(70\)90255-6](https://doi.org/10.1016/0022-1694(70)90255-6).

492 Pionke, H.B., Gburek, W.J., Sharpley, A.N., 2000. Critical source area controls on water quality in an

493 agricultural watershed located in the Chesapeake Basin. *Ecol. Eng.* 14(4), 325–335.
494 [https://doi.org/10.1016/S0925-8574\(99\)00059-2](https://doi.org/10.1016/S0925-8574(99)00059-2).

495 Qin, C.-Z., Gao, H.-R., Zhu, L.-J., Zhu, A.-X., Liu, J.-Z., Wu, H., 2018. Spatial optimization of watershed
496 best management practices based on slope position units. *J. Soil Water Conserv.* 73(5), 504–517.
497 <https://doi.org/10.2489/jswc.73.5.504>.

498 Rankinen, K., Keinänen, H., Cano Bernal, J.E., 2016. Influence of climate and land use changes on
499 nutrient fluxes from Finnish rivers to the Baltic Sea. *Agr. Ecosyst. Environ.* 216, 100–115.
500 <https://doi.org/10.1016/j.agee.2015.09.010>.

501 Rathjens, H., Bieger, K., Chaubey, I., Arnold, J.G., Allen, P.M., Srinivasan, R., Bosch, D.D., Volk, M.,
502 2016. Delineating floodplain and upland areas for hydrologic models: a comparison of methods.
503 *Hydrol. Process.* 30(23), 4367–4383. <https://doi.org/10.1002/hyp.10918>.

504 Rathjens, H., Oppelt, N., Bosch, D.D., Arnold, J.G., Volk, M., 2015. Development of a grid-based version
505 of the SWAT landscape model. *Hydrol. Process.* 29(6), 900–914. <https://doi.org/10.1002/hyp.10197>.

506 Shang, X., Wang, X., Zhang, D., Chen, W., Chen, X., Kong, H., 2012. An improved SWAT-based
507 computational framework for identifying critical source areas for agricultural pollution at the lake
508 basin scale. *Ecol. Model.* 226, 1–10. <https://doi.org/10.1016/j.ecolmodel.2011.11.030>.

509 Shen, Z., Zhong, Y., Huang, Q., Chen, L., 2015. Identifying non-point source priority management areas
510 in watersheds with multiple functional zones. *Water Res.* 68, 563–571.
511 <https://doi.org/10.1016/j.watres.2014.10.034>.

512 Shi, Y.-X., Zhu, L.-J., Qin, C.-Z., Zhu, A.-X., 2021. Spatial optimization of watershed best management
513 practices based on slope position-field units. *Journal of Geo-Information Science* 23(4), 564–575
514 (in Chinese with English abstract). <https://doi.org/10.12082/dqxxkx.2021.200335>.

515 Tian, F., Huang, J., Cui, Z., Gao, J., Wang, X., Wang, X., 2020. Integrating multi indices for identifying
516 priority management areas in lowland to control lake eutrophication: A case study in lake Gehu,
517 China. *Ecol. Indic.* 112, 106103. <https://doi.org/10.1016/j.ecolind.2020.106103>.

518 Volk, M., Arnold, J.G., Bosch, D.D., Allen, P.M., Green, C.H., 2007. Watershed configuration and
519 simulation of landscape processes with the SWAT model, in: MODSIM 2007 International Congress
520 on Modelling and Simulation. Modelling and Simulation Society of Australia and New Zealand,
521 Christchurch, New Zealand, pp. 2383–2389.

522 Wang, G., Chen, L., Huang, Q., Xiao, Y., Shen, Z., 2016. The influence of watershed subdivision level
523 on model assessment and identification of non-point source priority management areas. *Ecol. Eng.*
524 87, 110–119. <https://doi.org/10.1016/j.ecoleng.2015.11.041>.

525 White, M.J., Storm, D.E., Busteed, P.R., Stoodley, S.H., Phillips, S.J., 2009. Evaluating nonpoint source
526 critical source area contributions at the watershed scale. *J. Environ. Qual.* 38(4), 1654–1663.
527 <https://doi.org/10.2134/jeq2008.0375>.

528 Wolock, D.M., Winter, T.C., McMahon, G., 2004. Delineation and evaluation of hydrologic-landscape
529 regions in the United States using geographic information system tools and multivariate statistical
530 analyses. *Environ. Manage.* 34, S71–S88. <https://doi.org/10.1007/s00267-003-5077-9>.

531 Yang, D., Herath, S., Musiaka, K., 2002. A hillslope-based hydrological model using catchment area and
532 width functions. *Hydrolog. Sci. J.* 47(1), 49–65. <https://doi.org/10.1080/02626660209492907>.

533 Zhu, L.-J., Qin, C.-Z., Zhu, A.-X., 2021. Spatial optimization of watershed best management practice
534 scenarios based on boundary-adaptive configuration units. *Progress in Physical Geography: Earth
535 and Environment* 45(2), 207–227. <https://doi.org/10.1177/0309133320939002>.

536 Zhu, L.-J., Qin, C.-Z., Zhu, A.-X., Liu, J., Wu, H., 2019. Effects of different spatial configuration units

537 for the spatial optimization of watershed best management practice scenarios. *Water* 11(2), 262.

538 <https://doi.org/10.3390/w11020262>.

Table

Table 1. Data description of the study areas for building SWAT⁺.

	Zhongtianshe Watershed	<u>Willow River Watershed</u>
DEM	DEM with a resolution of 25 m from Provincial Geomatics Centre of Jiangsu	<u>DEM with a resolution of 30 m from National Elevation Data, USGS</u>
Land use	Manually interpreted from Google Earth image derived in 2015	<u>Land use map from National Land Cover Data (NLCD, 2011 Edition), USGS</u>
Soil	Soil type map obtained from Soil Science Database of China and soil properties from field sampling	<u>Soil dataset from the Soil Survey Geographic database (SSURGO), U.S. Department of Agriculture-Natural Resource Conservation Service</u>
Meteorological data	Daily meteorological data (such as precipitation, temperature, humidity, wind speed, and solar radiation) from 2011 to 2015 provided by China Meteorological Data Service Centre and Liyang meteorological station	<u>Daily meteorological data from 2008 to 2014 provided by Climate Forecast System Reanalysis dataset, U.S. National Centers for Environmental Prediction</u>
Agricultural management practices	Cropping and irrigation schedule including crop types and fertilizer usage from field survey	<u>Crop rotations, tillage practices and fertilizer usage collated from Almendinger and Murphy (2007)</u>
Observed data at the outlet	Daily measured flow (2011–2015) and 5-day measured total nitrogen data (2014–2015) from the site-monitoring station at the watershed outlet	<u>Daily flow and ammonia plus organic nitrogen data (from 1 October 2010 to 31 July 2014) measured at the monitoring station by USGS (no. 05341687)</u>

Table 2. The SWAT+ model performance of the two watersheds.

		<u>NSE</u>	<u>PBIAS</u>	<u>RSR</u>	<u>R²</u>	
<u>Zhongtianshe Watershed</u>	<u>Calibration</u>	<u>Flow</u>	<u>0.48</u>	<u>13.36%</u>	<u>0.72</u>	<u>0.52</u>
		<u>Nitrogen</u>	<u>0.27</u>	<u>-16.57%</u>	<u>0.86</u>	<u>0.40</u>
	<u>Validation</u>	<u>Flow</u>	<u>0.52</u>	<u>12.55%</u>	<u>0.69</u>	<u>0.59</u>
		<u>Nitrogen</u>	<u>=</u>	<u>=</u>	<u>=</u>	<u>=</u>
<u>Willow River Watershed</u>	<u>Calibration</u>	<u>Flow</u>	<u>0.48</u>	<u>-28.82%</u>	<u>0.72</u>	<u>0.51</u>
		<u>Nitrogen</u>	<u>0.37</u>	<u>3.97%</u>	<u>0.79</u>	<u>0.39</u>
	<u>Validation</u>	<u>Flow</u>	<u>0.34</u>	<u>-58.16%</u>	<u>0.81</u>	<u>0.47</u>
		<u>Nitrogen</u>	<u>0.25</u>	<u>-128.73%</u>	<u>0.87</u>	<u>0.54</u>

Figure

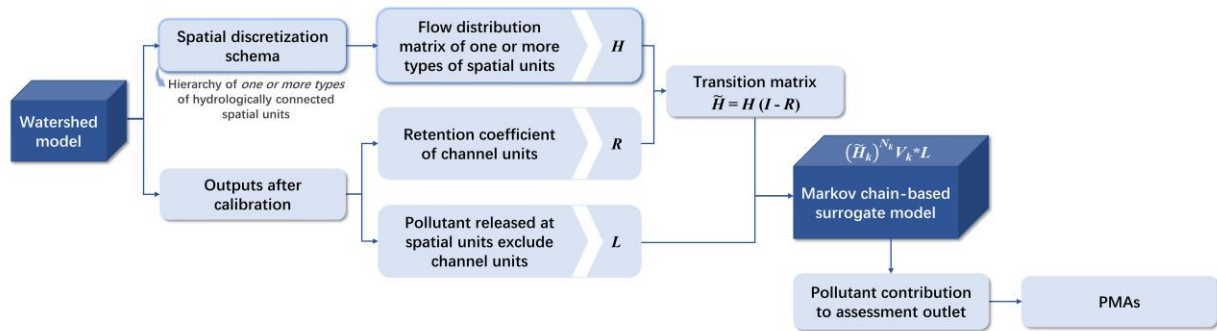


Fig. 1. Generalized framework of the Markov chain-based PMA identification method using a hierarchy of one or more types of hydrologically connected spatial units.

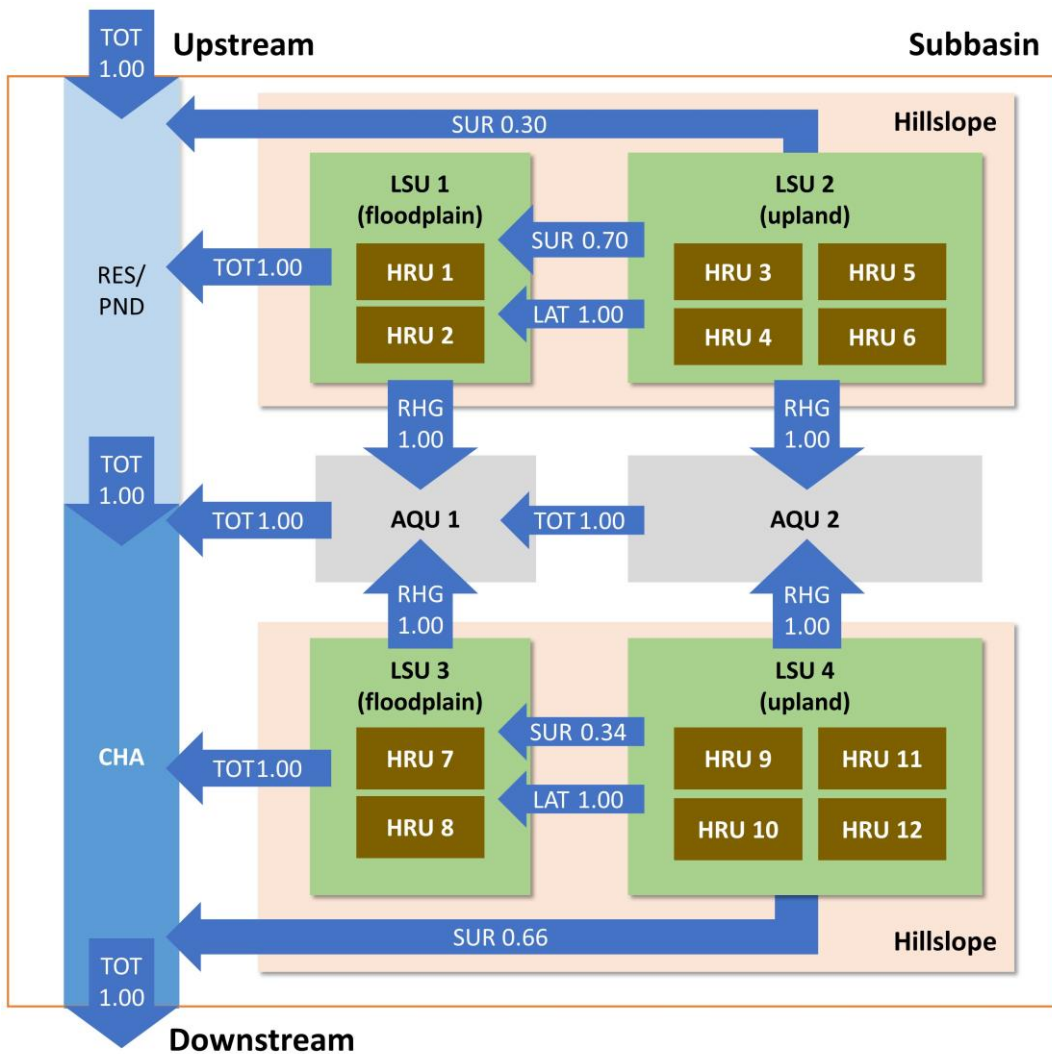


Fig. 2. **Schematic** of the spatial discretization scheme and hydrologic connections between spatial units implemented in SWAT+. AQU, aquifer; CHA, channel; HRU, hydrologic response unit; LSU, landscape position unit; LAT, lateral flow; PND, pond; RES, reservoir; RHG, groundwater recharge; SUR, surface runoff; TOT, total outflow (specifically, for LSU, it equals to surface runoff plus lateral flow); and numbers represent flow distribution ratio (**values less than 1.0 are presented for example**) from source unit to receiving unit (adapted from Bieger et al., 2017, 2019, and the source code of SWAT+ version 59.3).

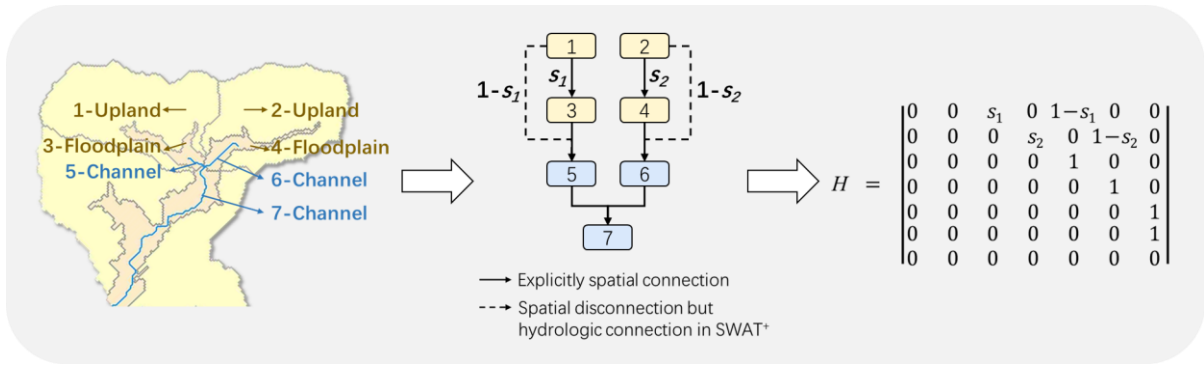


Fig. 3. Example of constructing flow distribution matrix H based on upstream-downstream relationships among landscape position units (LSUs) and channels and flow distribution ratios from upland to floodplain_ (e.g., s_1 and s_2 in different subbasins).

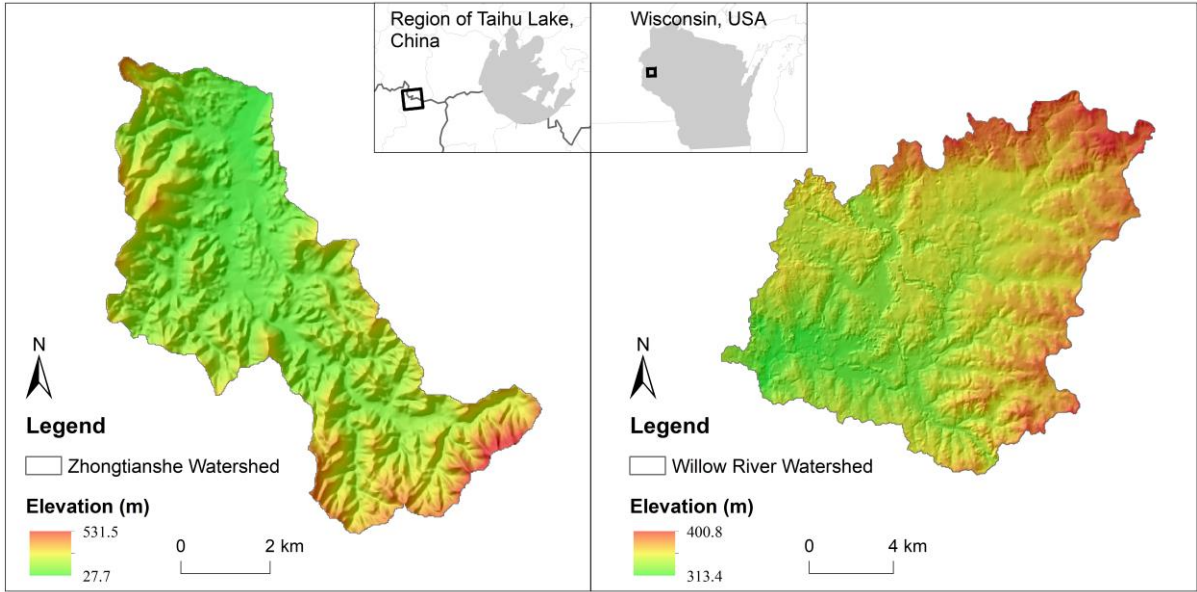


Fig. 4. Overview of the Zhongtianshe and Willow River Watersheds.

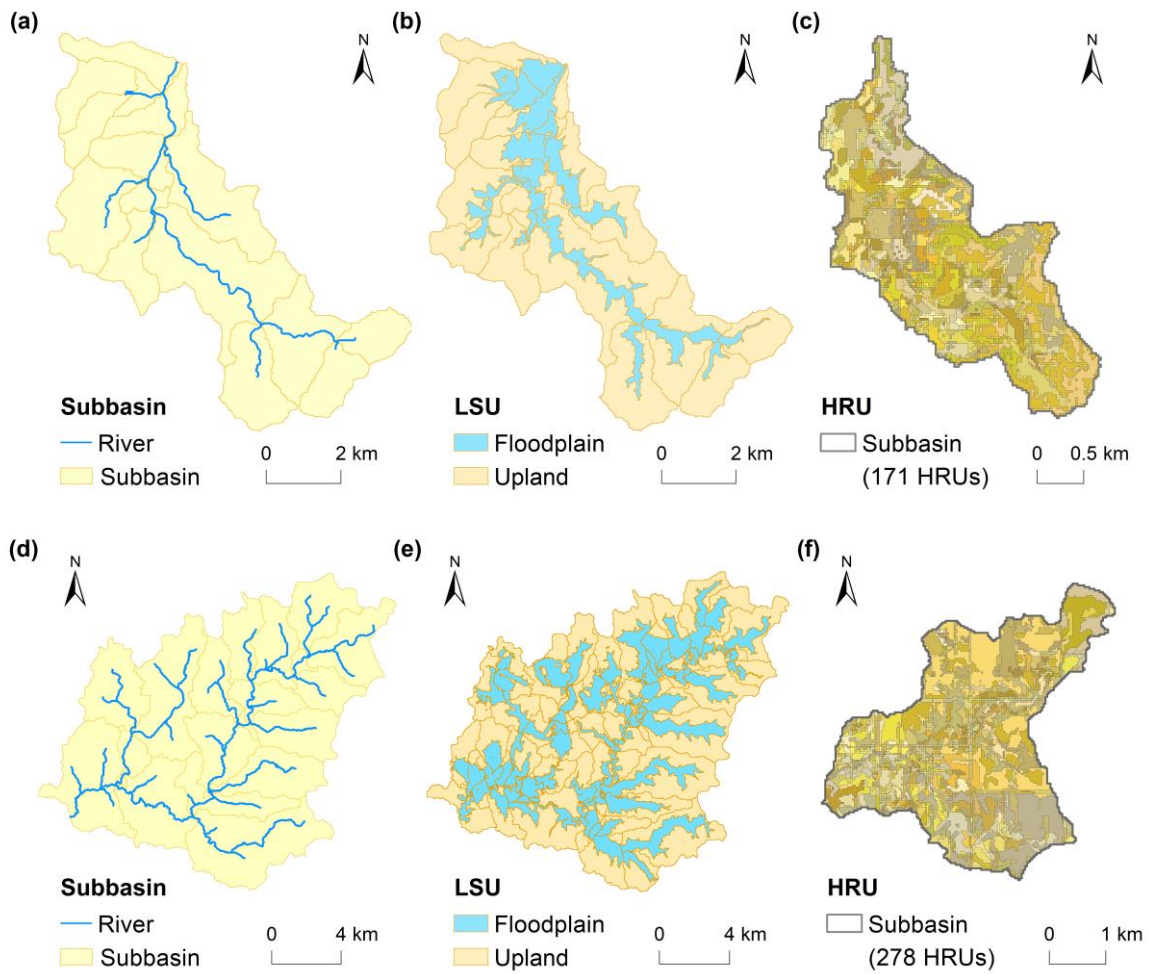


Fig. 5. Delineation of three types of spatial units in the SWAT⁺ model of the Zhongtianshe Watershed: (a) subbasin, (b) LSU, (c) HRU (take one subbasin as an example) and the Willow River Watershed: (d) subbasin, (e) LSU, (f) HRU (take one subbasin as an example). Each color within the same subbasin in the HRU map represents one unit, i.e., a particular combination of land use, soil type, and slope classification.

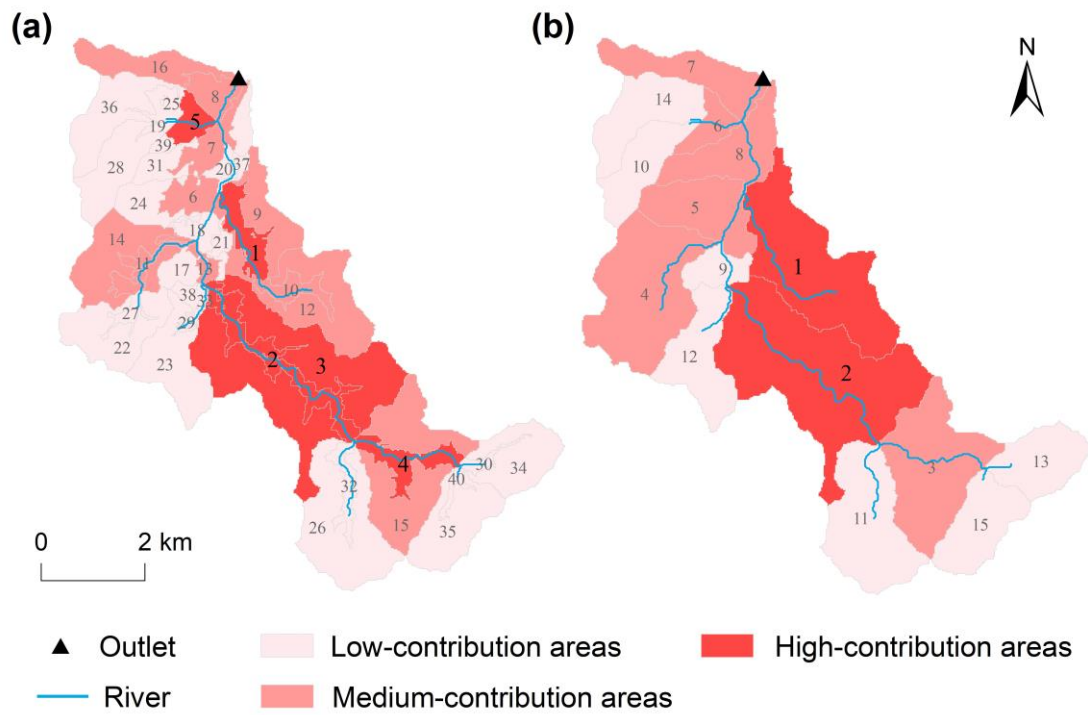


Fig. 6. Ranking and classification of nitrogen load contribution at the (a) LSU (landscape position unit) and (b) subbasin levels in the Zhongtianshe Watershed. The labelled number is the ranked sequence of load contribution in descending order. High-contribution areas are identified as PMAs.

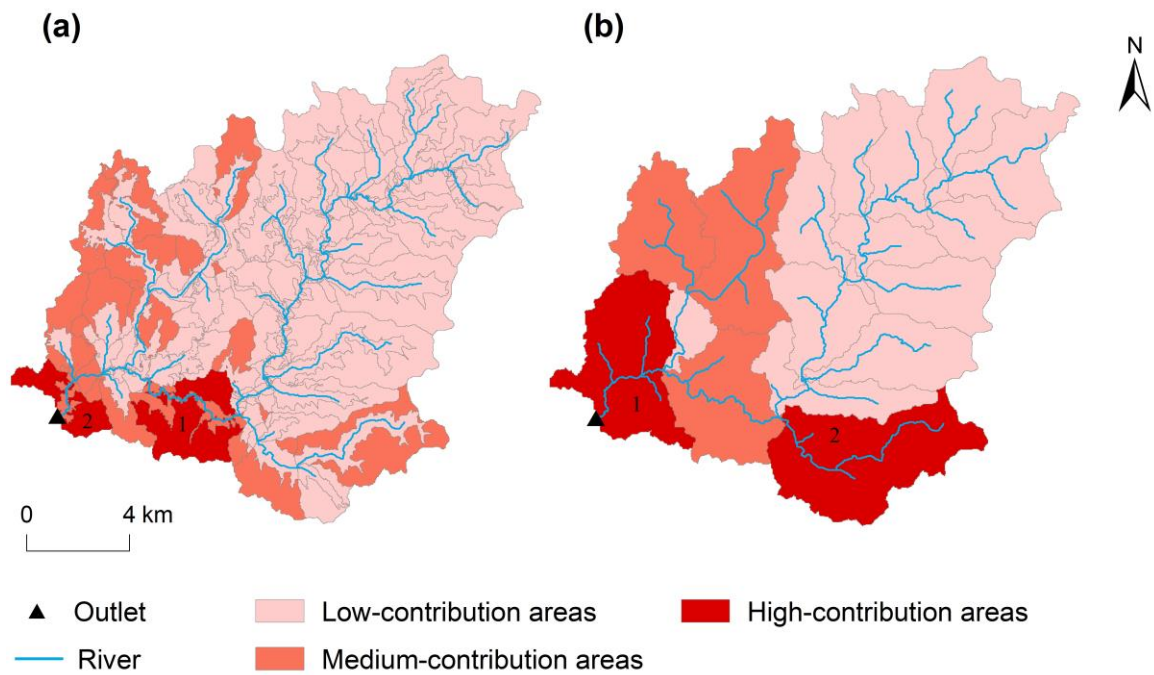


Fig. 7. Ranking and classification of total nitrogen load contribution at the (a) LSU (landscape position unit) and (b) subbasin levels in the Willow River Watershed. High-contribution areas are identified as PMAs, which are ranked and labelled by load contribution.

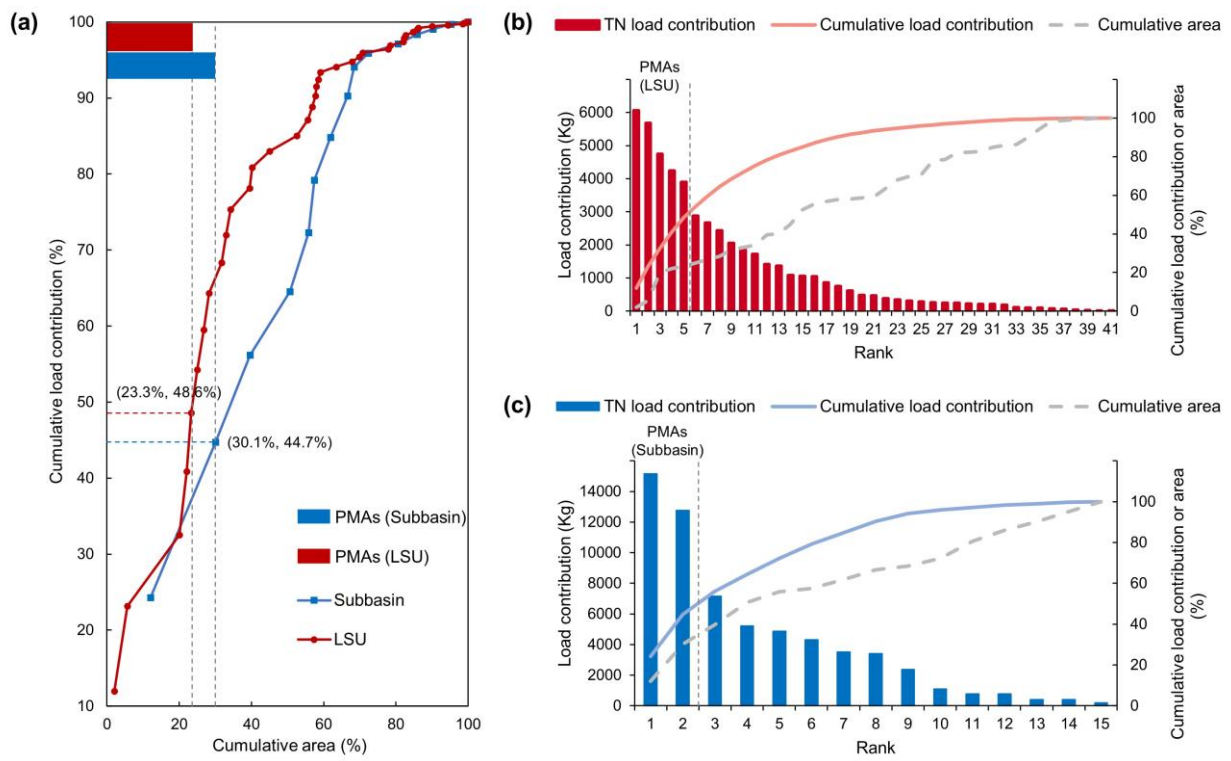


Fig. 8. Relationships between cumulative areas of spatial units and corresponding load contributions in the Zhongtianshe Watershed. (a) each point represents a spatial unit arranged in the descending order of load contribution. Detailed load contribution of landscape position units (LSUs) and subbasins are presented in (b) and (c), respectively.

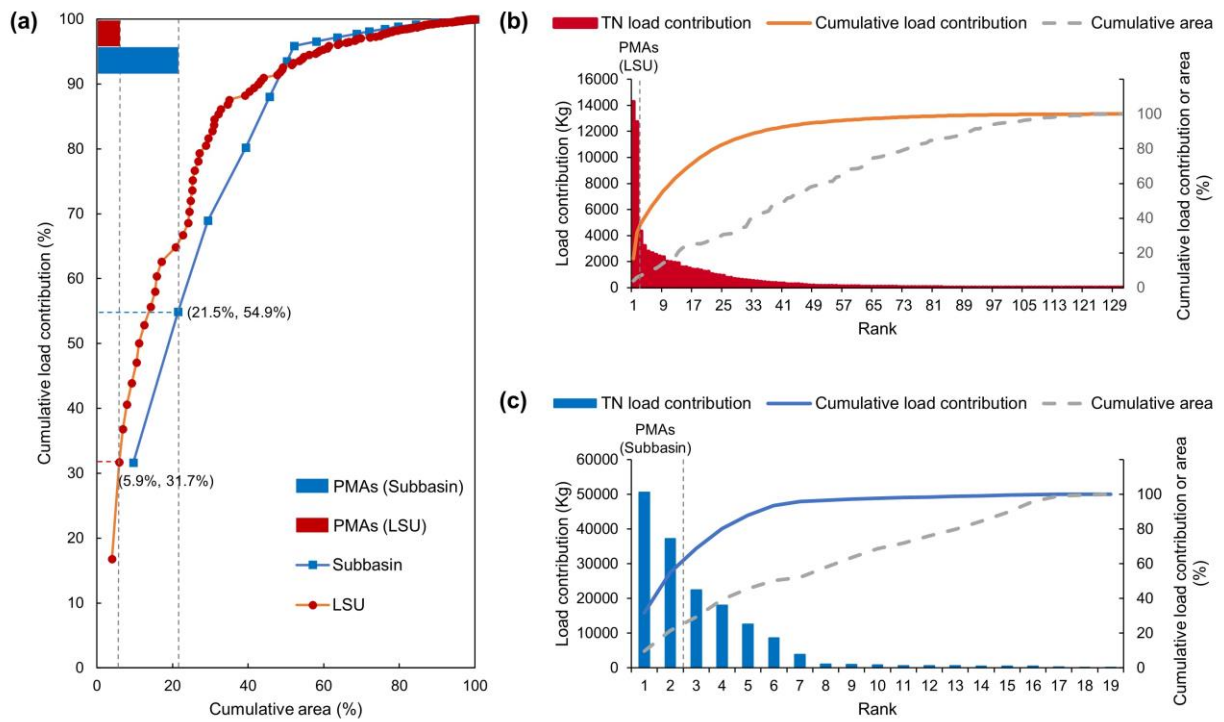


Fig. 9. Relationships between cumulative areas of spatial units and corresponding load contributions in the Willow River Watershed. (a) each point represents a spatial unit arranged in the descending order of load contribution. Detailed load contribution of landscape position units (LSUs) and subbasins are presented in (b) and (c), respectively.